Journal of Nuclear Materials 484 (2017) 270–275

Contents lists available at ScienceDirect

Journal of Nuclear Materials

journal homepage: www.elsevier.com/locate/jnucmat

# Trapping of hydrogen and helium at an {110}<111> edge dislocation in tungsten

Hongxian Xie [a, b, *], Ke Xu [c], Guang-Hong Lu [c, **], Tao Yu [d], Fuxing Yin [b, e]

[a] School of Mechanical Engineering, Hebei University of Technology, Tianjin 300132, China
[b] Tianjin Key Laboratory of Materials Laminating Fabrication and Interface Control Technology, Tianjin 300132, China
[c] School of Physics & Nuclear Energy Engineering, Beihang University, Beijing 100191, China
[d] Central Iron and Steel Research Institute, Beijing 100081, China
[e] Research Institute for Energy Equipment Materials, Hebei University of Technology, Tianjin 300132, China

ARTICLE INFO

*Article history:*
Received 11 May 2016
Received in revised form
12 October 2016
Accepted 15 December 2016
Available online 15 December 2016

ABSTRACT

We have performed an atomistic simulation to investigate energetics and dynamic behaviour of hydrogen (H) and helium (He) at an {110}<111> edge dislocation in tungsten (W). The edge dislocation is shown to attract H/He at the tensile stress region according to the negative interaction energy of H/He at the tensile stress region, which implies that the dislocation is energetically beneficial to accommodate both H and He. Dynamically both H and He are easy to diffuse into the dislocation core, indicating the 'down-hill' diffusion due to the presence of the dislocation serving as a trapping center for both H and He. Further, He exhibits much lower interaction energy and much faster diffusion into the dislocation core region as compared with H owing to the close shell electronic structure of He. The results suggest the edge dislocation as a trapping center facilitates the H/He accumulation, contributing to the understanding the role of the dislocation on the H/He accumulation and bubble formation in W.



## 1. Introduction

Due to its high melting point and good irradiation resistance tungsten (W) is the main candidate material for plasma facing components in future thermonuclear fusion reactors [1–4]. In an extreme fusion environment, W will be exposed to high fluxes of hydrogen (H) and helium (He) ions. The retention of H and He in W can lead to the formation of bubbles and their subsequent growth into sub-surfaces blisters [5–7]. A large accumulation of the bubbles will deteriorate the mechanical properties of W, induce the high-temperature embrittlement and surface erosion, and therefore give rise to important technological problem and reduce the life time of W. On the other hand, the retention of H and He particularly the surface blisters can largely affect the plasma stability because the core plasma can only accommodate W impurity no more than 20 appm [8,9]. It is thus quite important to explore the underlying mechanism of clustering, nucleation and growth of the H and He bubbles, so that we can propose the method to suppress or even remove the bubbles and to design the irradiation resistant W materials.

Defect in W such as vacancy and grain boundary is suggested as nucleation site for bubbles, and lots of experimental and theoretical works have been devoted to investigation of H bubble formation mediated by vacancy or grain boundary [10–19]. The vacancy mediated H bubble formation is proposed to be originated from a vacancy trapping mechanism [14,17]. When H atoms are trapped by the vacancy, they prefer to occupy the internal surface of the vacancy to form a "screening layer", which can screen the interaction between the further trapped H and the surrounding W atoms, making H stay at the vacancy center [14]. This leads to the formation of $H_2$ molecule at the vacancy center, which is considered to be the preliminary stage of H bubble nucleation. With H atoms continuously diffusing in, the H pressure will increase gradually, which leads to instability of the surrounding W lattice thus facilitating the creation of more vacancy to accommodate H atoms [20]. Such mechanism can be generated to other vacancy-related defects such as grain boundary [13].

In addition to vacancy and grain boundary, dislocation is also considered as the trapping center for H and He. Recently, the effect

* Corresponding author. School of Mechanical Engineering, Hebei University of Technology, Tianjin 300132, China.
** Corresponding author.
*E-mail addresses:* hongxianxie@163.com (H. Xie), LGH@buaa.edu.cn (G.-H. Lu).

http://dx.doi.org/10.1016/j.jnucmat.2016.12.014
0022-3115/

of dislocation on H and He accumulation and bubble formation has been paid a great attention. He bubble nucleation at low-angle twist boundaries in gold was investigated with transmission electron microscopy [21,22], in which the He bubbles were found to preferentially nucleate at screw dislocation nodal points, resulting in He bubble superlattice formation. High purity iron was irradiated *in situ* in a transmission electron microscope with 1 MeV $Fe^+$ ions while simultaneously implanting 15 keV $He^+$ ions, which reveals that a majority of He bubbles nucleates inside the large dislocation loops [23]. These experimental investigations demonstrate that dislocation has importantly effects on bubble formation. Computationally, the density functional theory investigation on the interaction of H with screw dislocation in Cu and dislocation loops in W shows that H binds strongly to the screw dislocation core and dislocation loops, which facilitates the bubble nucleation [24,25].

So far, however, only a few studies focused on the effects of dislocation on H/He clustering and bubble nucleation *in W*. Theoretically the role of the dislocation on H/He clustering and bubble nucleation has not been clarified. In particular, edge dislocation is another important line defect in addition to the screw dislocation. The edge dislocation has more vacant space than the screw dislocation, and thus can accommodate more H/He atoms beneficial to H/He accumulation and bubble formation. Here we have performed an atomistic simulation to investigate energetics and diffusion properties of H and He around an {110}<111> edge dislocation in W. The results will contribute to further understanding of the H/He accumulation and bubble nucleation in W.

## 2. Computational method

The supercell of the edge dislocation is shown in Fig. 1, in which *x*, *y* and *z* are set as the [111], [1−10], and [11−2] directions, respectively. Periodic boundary conditions are applied along the x and z directions. In order to introduce a 1/2<111>(1−10) edge dislocation, three (111) atomic planes along the *z* direction are removed from the middle of the supercell to the top surface, and then the relaxation of atomic structure is performed by the conjugate gradient method until the force on every atom was smaller than $10^{-9}$ eV/nm. The supercell contains 7776 W atoms, and the dimensions of the supercell are 9.85 nm, 8.06 nm and 1.55 nm along the x, y and z direction, respectively. Three atomic layers at the top and bottom of the supercell are considered as boundary layers and fixed. We have tested two systems with a larger size in the z directions (3.1 nm and 4.65 nm) and found that the size along z direction has little effect on the solute diffusion process and the interaction energy between the H/He atom and the edge dislocation.

It is well known that the computational results are strongly influenced by the characteristics of interatomic potential, and

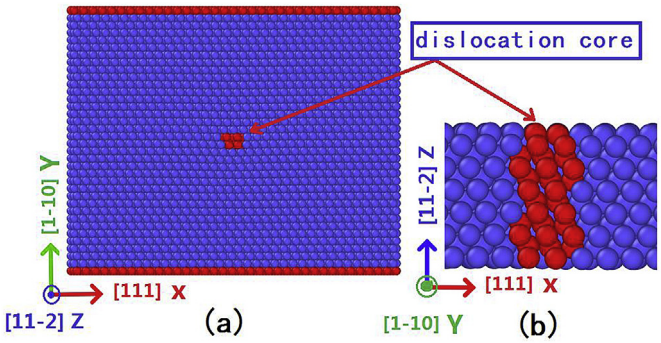


**Fig. 1.** Supercell of the {110}<111> edge dislocation. (a) side view (b) top view.

therefore the choice of the interatomic potential is extremely important. The self-developed analytical bond order potentials of W-H and W-He system [26,27] are employed, which reproduce various properties of the W-H-He system, including diffusion barriers and defect formation energies [28−31].

There are two types of H/He occupation sites within the body-centered cubic (bcc) lattice. One is the octahedral interstitial site (O site) and the other is the tetrahedral interstitial site (T site). The T site is the more stable occupation site for an H/He atom within the perfect body centered cubic (bcc) W [17,26,32]. However, the O site may become more stable in the largely deformed bcc-structure W (near the dislocation core area). Consequently, H/He are set at T sites within the prefect bcc lattice, while H/He are set at both T and O sites near the dislocation core with large lattice deformation.

## 3. Results and discussion

### 3.1. Stress distribution at the edge dislocation

We first determine the normal stress ($\sigma_{xx}$,$\sigma_{yy}$ and$\sigma_{zz}$), shear stress ($\sigma_{xy}$) and average normal stress ($\sigma_a$) of each atom near the edge dislocation. The stress of each atom is calculated in a virial form, and the average stress of each atom is determined by$(\sigma_{xx}+\sigma_{yy}+\sigma_{zz})/3$. The calculated stress distribution at the edge dislocation is shown in Fig. 2, which clearly gives two different stress regions, i.e. tensile-stress region and compressive-stress region, at the edge dislocation core, and shear stress along the slipping plane of the dislocation. Such stress distribution at the edge dislocation agrees well with the distribution from the classical linear elasticity equations [33]. Moreover, the stress values near the dislocation core are very high and even reach a few GPa, which will surely remarkably affect the distribution of H/He at the edge dislocation.

### 3.2. Energetics of H at the edge dislocation

In order to investigate the interaction between H and the edge dislocation, we next calculate the interaction energy between H atom and the dislocation at different occupation sites at the edge dislocation. Via setting an H atom at certain interstitial site, and then relaxing the atomic structure by the CG method, the interaction energy of H with the dislocation is calculated by

$$\Delta E_1 = \left[E_{(d,H)} - E_d - \frac{1}{2}E_{H_2}\right] - E_0, \tag{1}$$

where $E_{(d,H)}$ and $E_d$ are the potential energy of the dislocation system with and without an H atom, $E_{H_2}$ is the potential energy of an H molecule, and $E_0$ is the solution heat of the H atom at the T site in the W perfect lattice with a value of 0.86 eV [27].

Fig. 3 shows the interaction energy distribution at the dislocation core. Here, we set an H atom in region *A* (the slipping plane of the edge dislocation) and region *B* [Fig. 3(a)], then calculate the interaction energies [Fig. 3(b)]. We discuss region B first. When the H atom is placed in the upper part of the region B (tensile region of the edge dislocation), the interaction energy is negative. With H closer to the dislocation core, the interaction energy becomes more negative. H at the dislocation core exhibits the lowest interaction energy, which is −1.53 eV. On the other hand, when the H atom is placed in the lower part of the region B (compressive region of the edge dislocation), the interaction energy is positive. With H closer to the dislocation core, the interaction energy becomes more positive, with the highest interaction energy of +0.76 eV. This indicates that the tensile region at the edge

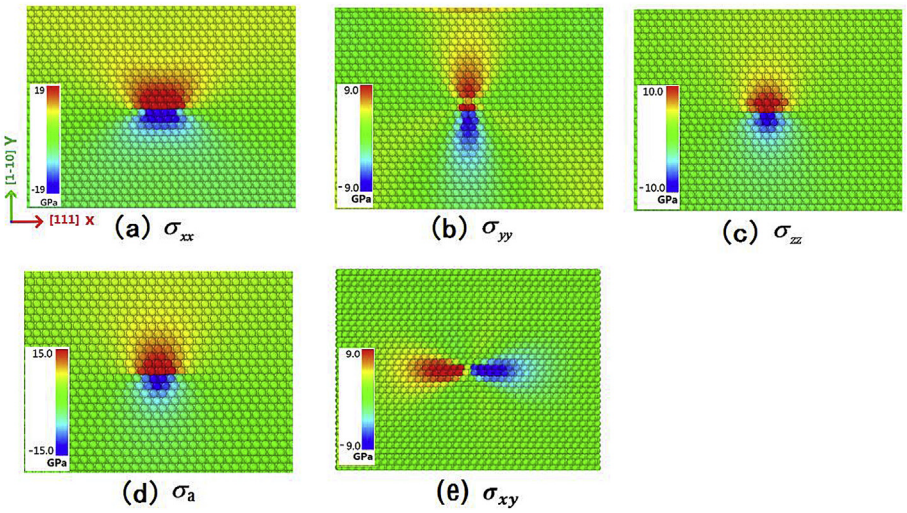


**Fig. 2.** Stress distribution at the {110}<111> edge dislocation. (a), (b) and (c) display the normal stress along the x, y and z directions, respectively; (d) displays the average stress, (e) displays the shear stress.

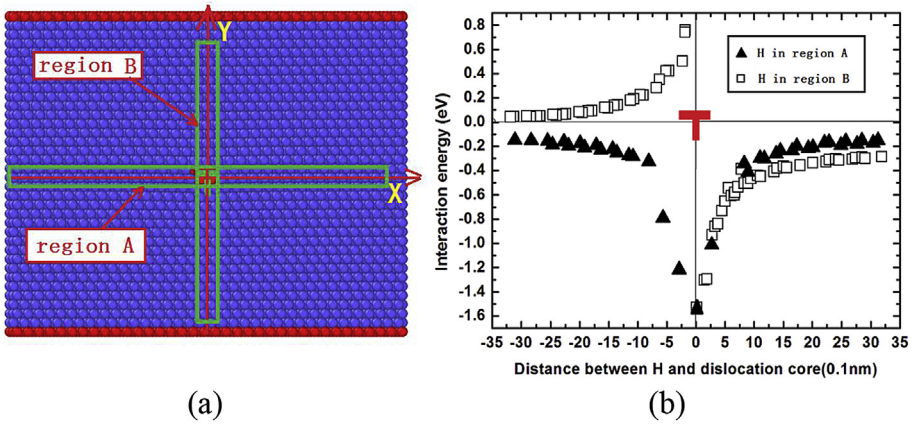


**Fig. 3.** The distribution of H-dislocation interaction energy at the edge dislocation. (a) indicates the region A (along the x direction, the slipping plane of the edge dislocation) and region B (along the y direction), at which the interaction energy of H/He with the dislocation is calculated. Note that the dislocation is set at origin of coordinate. (b) shows the distribution of the H-dislocation interaction energy at the region A and B.

dislocation attracts H atom while the compressive region repels H. This is consistent with the stress distribution at the dislocation shown in Fig. 2.

When the H atom is placed in region A, the interaction energy is all negative, which indicates that the edge dislocation can attract the H atom in region A. Such attraction effect can be enhanced with H atom closer to the dislocation. Again, H at the dislocation core exhibits the lowest interaction energy, −1.53 eV. The negative interaction energy between H atom and dislocation is a much novel and strange phenomenon because there is not normal stress along the slip plane. However, we notice that there exist large shear stress (Fig. 2(e)), which suggests that the interaction energy between H and the edge dislocation is also sensitive to shear stress. The effect of shear stress on the interaction energy between H and dislocation is first discovered by R. Matsumoto et al. during studying the H distribution and diffusion around an edge dislocation in bcc iron [34], and then is further calculated and discussed by using density functional theory [35]. In the present work, we verify that the shear stress also has effect on the interaction energy between H and edge dislocation in bcc W.

### 3.3. Energetics of He at the edge dislocation

Similar to the H case, the interaction energy of He with the dislocation is calculated by

$$\Delta E_2 = \left[E_{(d,He)} - E_d - E_{He}\right] - E_1, \tag{2}$$

where $E_{(d,He)}$ and $E_d$ are the potential energy of the dislocation system with and without an He atom, $E_{He}$ is the potential energy of an He atom, and $E_1$ is the solution heat of the He atom at the T site in the W perfect lattice with a value of 6.21 eV.

Fig. 4 shows the interaction energy distribution at the dislocation core. Here, similar to the H case, we set He at region *A* and region *B* as shown in Fig. 3(a) to calculate the He-dislocation interaction energy. Basically the interaction energy results are similar to the H case. However, because of the close-shell electronic structure, He should exhibit stronger stress effect of interaction energy with dislocation. This is clearly reflected in the interaction energy results of He.

As shown in Fig. 4, when the He atom is placed in the upper part

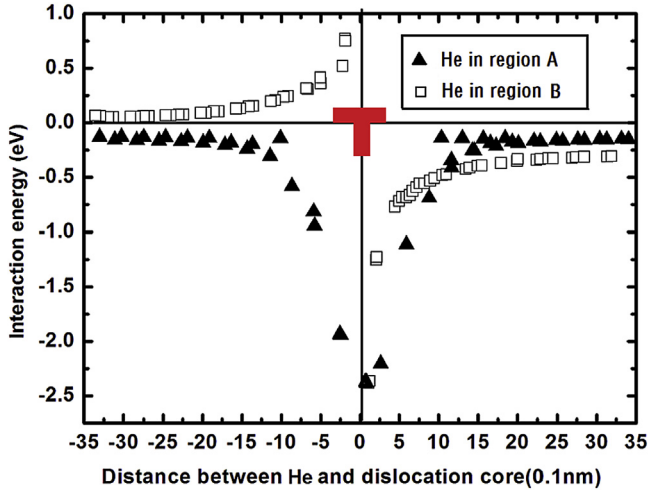


**Fig. 4.** The distribution of He-dislocation interaction energy at the region A and B.

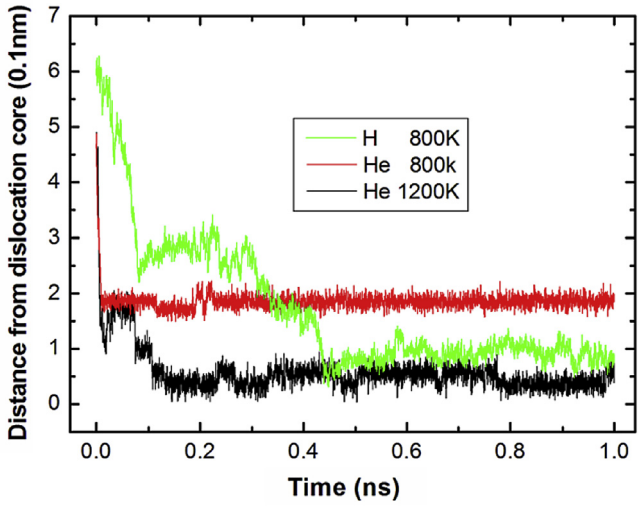


**Fig. 5.** The distance between the dislocation core and the mass center of the H/He atoms during diffusion process.

of the region B (tensile region of the edge dislocation), the interaction energy is negative. The lowest interaction energy value is −2.38 eV, much lower than −1.53 eV of the H case. When the He atom is placed in the lower part of the region B (compressive region of the edge dislocation), the interaction energy is positive. This also indicates that the tensile region at the edge dislocation attracts He atom while the compressive region repels He. On the other hand, when the He atom is placed in region A, the interaction energy is negative until the value is −2.38 eV, indicating the attraction effect is enhanced with He atom closer to the dislocation. Additionally, the shear stress also has effect on the interaction energy between He and edge dislocation in bcc W.

### 3.4. H and He diffusion at the edge dislocation core

We perform molecular dynamics (MD) simulation to investigate the H/He diffusion behaviour at the edge dislocation. The geometry of the MD model is the same as that in the molecular statics analyses (Fig. 1). Based on the above energetic results of H and He, originally ten H/He atoms are randomly introduced at different positions in the tensile region of the edge dislocation, and the distances between the H/He atoms and dislocation core are set to be not larger than 1.5 nm. The MD simulation is conducted for 1.0 ns with a time step of 0.2 fs During the diffusion process, the distance between the dislocation core and the mass center of the ten H/He atoms is calculated, as shown in Fig. 5. The initial distances of the H and He atoms are calculated to be 0.63 nm and 0.49 nm, respectively.

Fig. 5 shows the distance decreases with the increasing time, indicating that both H and He atoms diffuse towards the dislocation core. He is shown to diffuse much faster than H at the temperature of 800 K. This is because that the diffusion barrier of He (0.02–0.06 eV) is much lower than that of H (0.20–0.23 eV) [26,27,32,36]. At the time of 0.45 ns, the distance of H atoms converges to ~0.05 nm, indicating that the H atoms reach and are trapped at the dislocation core region. Different from H, He diffuses quickly towards the dislocation core region, but converges surprisingly to the distance ~0.18 nm from the dislocation core. If we increase the simulation temperature to 1200 K, the He atoms diffuse quickly into the dislocation core, characterized by convergence of the distance to ~0.05 nm at the time of 0.15 ns.

To further understand the strange diffusion behaviour of He at 800 K, we investigate variation of the atomic configuration as a function of time as displayed in Fig. 6. Originally three He atoms sit at the dislocation core region, while seven others sit outside the core region. At 0.005 ns, two more He atoms gather at the dislocation core area, as shown in Fig. 6(b). With time evolving to 0.014 ns, another two He atoms arrive at the dislocation core region. However, the rest three He atoms gather together to form an He cluster, which is not able to diffuse into the dislocation core region even at the time of 1.0 ns (Fig. 6(d)). The reason lies in that the diffusion barrier of the He cluster should be much higher than that of single He atom [37]. Such He cluster is stable. The cluster remains unchanged even the temperature is further elevated from 800 K to 1200 K with the evolution time of 1 ns This is again originated from the close-shell electronic structure of He, making it easy to cluster with each other.

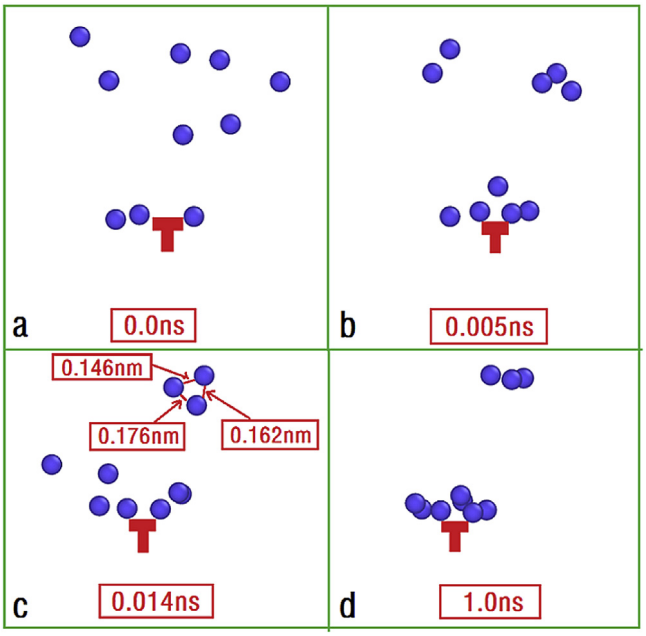


**Fig. 6.** Atomic configuration of He as a function of time evolution at temperature of 800 K. The blue spheres represent He atoms. (For interpretation of the references to colour in this figure legend, the reader is referred to the web version of this article.)

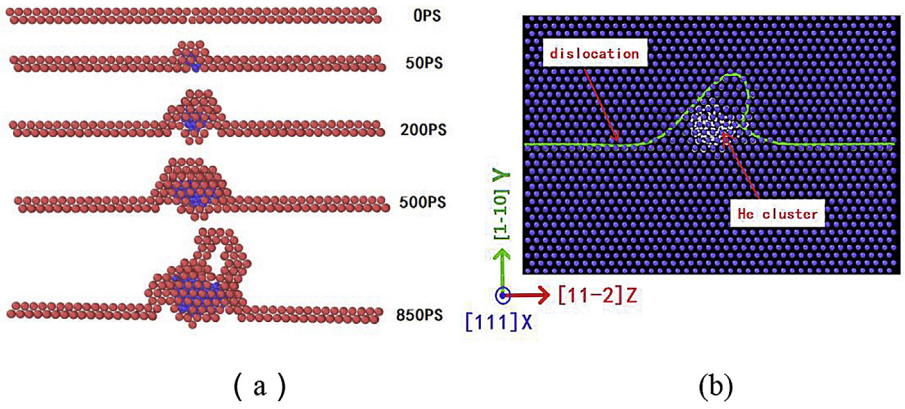


**Fig. 7.** The growth mechanism of He cluster in the edge dislocation core.

According to Sievert's law [38], the equilibrium concentration of H/He is proportional to $p^{\frac{1}{2}}$, where $p$ is the H/He gas pressure. This is to say that if we want to calculate the solute atom equilibrium concentration we must know the value of H/He gas pressure first. By now it is difficult to obtain the H/He pressure in thermonuclear fusion reactors; therefore, in the present work we don't calculate the solute atom equilibrium concentration.

### *3.5. The growing mechanism of He cluster in the edge dislocation core*

In this part, the effect of edge dislocation on the growing mechanism of a He cluster is studied. The new supercell is obtained by expanding original supercell (Fig. 1) seven times along z direction, contains 54432 W atoms. Then He atoms is introduced one by one into the middle part of the edge dislocation core. After each He atom is introduced, the supercell is relaxed for 5ps using the NVT ensemble (300 K). When He atoms are introduced in the dislocation core, they will gather at the tensile stress region of the dislocation core and form a small He cluster, which pushes a part of edge dislocation climbs towards tensile stress region, and leading to produce a jog on the edge dislocation (50ps in Fig. 7(b)). This growing mechanism is very similar to the growing mechanism of H cluster in a screw dislocation core [39]. With more He atoms are introduced, the edge dislocation climbs towards tensile stress region further, and leading the jog grows larger (200ps and 500ps). By the end of 850ps, the edge dislocation has climbed 2.2 nm towards tensile stress region and a big jog is formed on the edge dislocation. To display the jog clearly, the dislocation is identified by using the extraction algorithm (DXA) method [40] and display the results in Fig. 7(b), from which it can be found clearly that a big jog on the edge dislocation is pushed out by the He cluster.

## 4. Summary

In summary, energetics and dynamic behaviour of hydrogen (H) and helium (He) at an {110}<111> edge dislocation in tungsten (W) have been investigated using an atomistic simulation method. The edge dislocation is shown to attract H/He at the tensile stress region and repel H/He at the compressive stress region according to the negative (positive) interaction energy of H/He at the tensile (compressive) stress region. The dislocation is thus energetically beneficial to accommodate both H and He. These H and He are capable of diffusing towards the dislocation core region, which serves as a trapping center for both H and He. Further, H and He behaves differently at the dislocation due to different electronic structures. In comparison with H, He exhibits much lower interaction energy with dislocation (−2.38 eV/He vs. −1.53 eV/H), and much faster diffusion into the dislocation core region, owing to characteristics of He with the close shell electronic structure. The results suggest the edge dislocation facilitates the H/He accumulation and the bubble nucleation, contributing to the understanding the role of the dislocation on the H/He accumulation and bubble formation. The effect of edge dislocation on the growing mechanism of a He cluster is also studied, and it is found that the growing mechanism is by pushing out a jog on the edge dislocation.

## Acknowledgments

This work was supported by the Natural Science Foundation of China (Grant No. 51571082) and the National Magnetic Confinement Fusion Program of China (Grant No. 2013CB109002). G.H. Lu thanks the support from the Natural Science Foundation of China (Grant No.51325103, Distinguished Young Scholars).

## References

[1] G. Janeschitz, ITER JCT and HTs, J. Nucl. Mater. 290 (2001) 1.
[2] G. Federici, et al., J. Nucl. Mater. 313 (2003) 11.
[3] K. Tobita, et al., Fusion Eng. Des. 81 (2006) 1151.
[4] H.D.B. enkins, H.K. Roobottom, CRC Handbook of Chemistry and Physics, 85th edn, CRC Press, Boca Raton, FL, 2004.
[5] M. Fukumoto, Y. Ohtsuka, Y. Ueda, M. Taniguchi, M. Kashiwagi, T. Inoue, K. Sakamoto, J. Nucl. Mater. 375 (2008) 224.
[6] G.-N. Luo, W.M. Shu, M. Nishi, J. Nucl. Mater. 347 (2005) 111.
[7] F.S. Liu, Y. Zhang, W.J. Han, J.G. Yu, G.H. Lu, K.G. Zhu, Nucl. Instrum. Methods Phys. Res. B 307 (2013) 320.
[8] V. Philipps, J. Nucl. Mater 415 (2011) S2.
[9] G. Federici, et al., Nucl. Fusion 41 (2001) 1967.
[10] R.A. Causey, J. Nucl. Mater. 300 (2002) 91.
[11] W.M. Shu, G.-N. Luo, T. Yamanishi, J. Nucl. Mater 367–370 (2007) 1463.
[12] W.M. Shu, A. Kawasuso, T. Yamanishi, J. Nucl. Mater 386–388 (2009) 356.
[13] H.B. Zhou, Y.L. Liu, S. Jin, Y. Zhang, G.N. Luo, G.H. Lu, Nucl. Fusion 50 (2010) 025016.
[14] L. Sun, S. Jin, X.C. Li, Y. Zhang, G.H. Lu, J. Nucl. Mater 434 (2013) 395.
[15] G.H. Lu, H.B. Zhou, S.B. Charlotte, Nucl. Fusion 54 (2014) 086001.
[16] O. El-Atwani, K. Hattar, J.A. Hinks, G. Greaves, S.S. Harilal, A. Hassanein, J. Nucl. Mater 458 (2015) 216.
[17] Y.L. Liu, Y. Zhang, H.B. Zhou, G.H. Lu, Phys. Rev. B 79 (2009) 172103.
[18] K. Ohsawa, J. Goto, M. Yamakami, M. Yamaguchi, M. Yagi, Phys. Rev. B 82 (2010) 184117.
[19] K. Ohsawa, K. Eguchi, H. Watanabe, M. Yamaguchi, M. Yagi, Phys. Rev. B 85 (2012) 094102.
[20] S.Y. Qin, S. Jin, L. Sun, H.B. Zhou, Y. Zhang, G.H. Lu, J. Nucl. Mater 465 (2015) 135.
[21] J. Hetherly, E. Martinez, Z.F. Di, M. Nastasi, A. Caro, Scr. Mater. 66 (2012) 17.
[22] Z.F. Di, X.M. Bai, Q.G. Wei, J.H. Won, R.G. Hoagland, Y.Q. Wang, A. Misra, Phys. Rev. B 84 (2011) 052101.
[23] D. Brimbal, B. Décamps, A. Barbu, E. Meslin, J. Henry, J. Nucl. Mater 418 (2011) 313.
[24] D. Terentyev, V. Dubinko, A. Bakaev, Y. Zayachuk, W.V. Renterghem, P. Grigorev, Nucl. Fusion 54 (2014) 042004.

[25] W. Xiao, W.T. Geng, J. Nucl. Mater 430 (2012) 132–136.
[26] X.C. Li, X.L. Shu, Y.N. Liu, Yi Yu, F. Gao, G.H. Lu, J. Nucl. Mater 426 (2012) 31–37.
[27] X.C. Li, X.L. Shu, Y.N. Liu, F. Gao, G.H. Lu, J. Nucl. Mater 408 (2011) 12–17.
[28] X.G. Yu, F.J. Gou, T. Xia, J. Nucl. Mater 441 (2013) 324.
[29] X.G. Yu, F.J. Gou, Plasma Sci. Technol. 7 (2013) 710.
[30] Y. Yu, X.L. Shu, Y.N. Liu, G.H. Lu, J. Nucl. Mater 455 (2014) 91. http://www.sciencedirect.com/science/article/pii/S0022311514002281-cor1.
[31] P.M. Piaggi, et al., J. Nucl. Mater 458 (2015) 233.
[32] Y.L. Liu, Y. Zhang, G.N. Luo, G.H. Lu, J. Nucl. Mater. 390–391 (2009) 1032.
[33] J.P. Hirth, Theory of Dislocations, second ed., McGraw-Hill, New York, 1982.
[34] Shinya Taketomi, Ryosuke Matsumoto, Noriyuki Miyazaki, Acta Mater. 56 (2008) 3761.
[35] Ryosuke Matsumoto, Yoshinori Inoue, Shinya Taketomi, Noriyuki Miyazaki, Scr. Mater 60 (2009) 555.
[36] C.S. Becquart, C. Domain, Phys. Rev. Lett. 97 (2006) 196402.
[37] X.C. Li, et al., J. Nucl. Mater 455 (2014) 544.
[38] Shinya Taketomi, Ryosuke Matsumoto, Noriyuki Miyazaki, Int. J. Mech. Sci. 52 (2010) 334.
[39] D. Terentyev, V. Dubinko, A. Bakaev, Y. Zayachuk, W. Van Renterghem1, P. Grigorev, Nucl. Fusion 54 (2014) 042004.
[40] A. Stukowski, V.V. Bulatov, A. Arsenlis, Model. Simul. Mater. Sci. Eng. 20 (2012) 085007.